MoM ANALYSIS OF A CIRCULARLY POLARIZED CONICAL BEAM SPHERICAL SLOT ARRAY ANTENNA

Chuwong PHONGCHAROENPANICH†, Monai KRAIRIKSH†, and Jun-ichi TAKADA‡
†Faculty of Engineering and Research Center for Communications and Information Technology, King Mongkut's Institute of Technology Ladkrabang, Bangkok 10520 Thailand
Phone: (662) 3269967 Ext.3342 Fax: (662) 3269086 E-mail: kpchuwon@kmitl.ac.th
‡International Cooperation Center for Science and Technology, Tokyo Institute of Technology, Tokyo, 152-8550, Japan, Email: takada@icc.titech.ac.jp

1. Introduction

A circularly polarized conical beam spherical slot array antenna is proposed for the application of the low bit rate or low gain over temperature ratio (G/T) land mobile satellite communication subscriber and broadcasting service in addition to the wireless Local Area Network base station [1], [2]. The advantage of this antenna type is that the structure is simple and suitable for mass production i.e., a ring of perpendicular slot pairs cut on an outer surface of the concentric conducting spherical cavity enclosed by the conducting conical surface. The feeding structure is also simple, a linear electric probe excited at the center of the inner surface of the cavity to generate axially symmetrical mode, and it is integrated with the power divider. From the preliminary results of external radiation characteristic investigations [2], the radiation pattern appears to be the conical beam i.e., the elevation pattern possesses the null in broadside direction and the azimuthal pattern is omnidirectional. Additionally, the elevational beam direction toward the geostationary satellite is relatively low which is suitable for applying to the land mobile subscriber unit located far from the equator. However, to transfer the power from a transmitter to the antenna or the antenna to a receiver efficiently, impedance characteristics of the antenna should be estimated in order that appropriate matching is accomplished. Therefore, phenomena of the field inside the cavity in conjunction with outside the cavity must be taken into account. Method of moments plays an important role in solving unknown current of integral equations. The system of integral equations is formulated by enforcing the boundary condition that the tangential magnetic fields inside and outside the cavity are continuous through the slot aperture and the source model is considered at bottom of the feed probe. Using the aids of the dyadic Green's function in conjunction with the method of moments, the impedance and radiation characteristics are realized. Experimental results verified the theoretical ones.

2. Antenna Structure

The structure of a circularly polarized conical beam spherical slot array antenna consists of a number of perpendicular slot pairs cut on an outer surface of a concentric conducting spherical cavity enclosed by the conducting conical surface as shown in Fig.1. The slots in a pair are excited with orthogonal phases to provide the circularly polarized radiation. These slots are arranged as a ring along an azimuthal circumference of the spherical surface at the positions where the adjacent pairs are in phase to form a conical beam. Figure 1(a) shows the perspective view of the circularly polarized conical beam spherical slot array antenna. The slot length and width are l_s and ε_s, respectively. Each slot in a pair is separated, along an elevation plane d_θ, at the distance so that the phase quadrature is obtained [3]. The azimuthal spacing between each slot pair is denoted by s_ϕ. One of the slots in a pair is oriented at $45°$ counterclockwise with the horizontal line of the spherical surface whereas the perpendicular counterpart is oriented at an angle of $135°$. The cross-section view of the antenna is shown in Fig.1 (b). The inner and outer radii of the concentric conducting spherical cavity are R_a and R_b, respectively, and this cavity is enclosed by the conducting conical surface at an angle θ_c. The excitation probe is located at the center of the inner surface of the cavity ($R_a \le R \le R_b$, $\theta=0°,\phi=0°$). The center of each slot pair is located at an angle θ_s. Each slot in a pair is offset from the position in opposite direction so that phase quadrature between these slots is obtained.

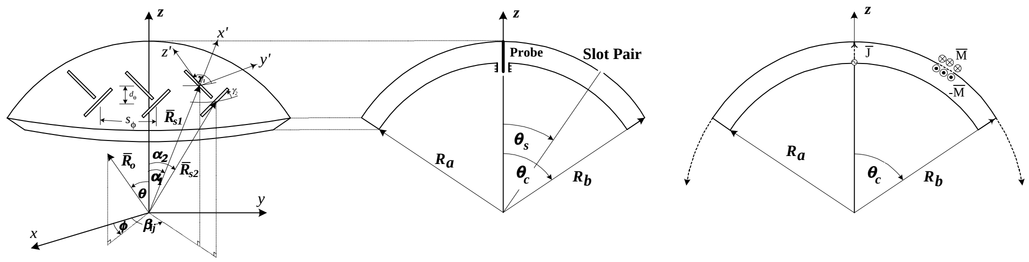

(a) (b) (c)

Fig 1 A circularly polarized conical beam spherical slot array antenna
(a) perspective view (b) cross-section view (c) Equivalent model

3. Analysis

3.1 Equivalent model

To realize the characteristics of the antenna, the integral equations of the unknown magnetic currents over the slots and electric current at the feed probe must be established. These equations are formulated base on the Field Equivalent Principle and enforcing the boundary condition as follows:

(i) Tangential magnetic fields are continuous through the slot aperture.

(ii) The delta gap source is considered at the bottom of the feed probe.

The equivalent model corresponds to the antenna configuration as in Fig. 1(b) is illustrated as in Fig.1(c).

3.2 Formulations

Applying the Galerkin's method of moments, the following linear equations for unknown coefficients v_{sk} and a_f are obtained. The time harmonic $e^{-i\omega t}$ is used and suppressed throughout the paper.

$$i\omega\varepsilon_o\sum_{k=1}^{N_s}v_{sk}\left\{\iint_{sl}\iint_{sk}(\hat{e}_{sl}\times\hat{r})\cdot\left(\overline{\overline{G}}{}^{in}_{HM}+\overline{\overline{G}}{}^{out}_{HM}\right)\cdot(\hat{e}_{sk}\times\hat{r})dS_{sk}dS_{sl}\right\}-a_f\iint_{sl}\int_f(\hat{e}_{sl}\times\hat{r})\cdot\overline{\overline{G}}{}^{in}_{HJ}\cdot\hat{j}_f dl_f dS_{sl}=0 \tag{1}$$

$$-\sum_{k=1}^{N_s}v_{sk}\int_f\iint_{sk}\hat{j}_f\cdot\overline{\overline{G}}{}^{in}_{EM}\cdot(\hat{e}_{sk}\times\hat{r})dS_{sk}dl_f+i\omega\mu_o a_f\int_f\int_f\hat{j}_f\cdot\overline{\overline{G}}{}^{in}_{EJ}\cdot\hat{j}_f dl_f dl_f=-1 \tag{2}$$

where $l=1,2,\ldots,N_s$. The dyadic Green's functions inside and outside the concentric conducting spherical cavity enclosed by the conducting conical surface for electric and magnetic fields due to the electric and magnetic current sources are derived [4], [5] to fulfill the requirement of the integral equations. The results are

$$\begin{aligned}G^{in}_{HM,\theta\theta}=&\frac{1}{k^2}\sum_{l=1}^{\infty}\sum_{m=1}^{\infty}A_o\Big[\sum_{\lambda=m}^{\infty}\frac{1}{(\kappa_p^2-k^2)I_{\lambda p}}\frac{1}{rr'}\Re'_\lambda(r)\Re'_\lambda(r')\Theta'_\lambda(\theta)\Theta'_\lambda(\theta')\Phi_1(\phi)\Phi_1(\phi')\\&+\sum_{\mu=m}^{\infty}\frac{\kappa_q^{\ 2}}{(\kappa_q^2-k^2)I_{\mu q}}\frac{m^2}{sin\theta sin\theta'}\Re_\mu(r)\Re_\mu(r')\Theta_\mu(\theta)\Theta_\mu(\theta')\Phi_2(\phi)\Phi_2(\phi')\Big]\end{aligned} \tag{3}$$

$$\begin{aligned}G^{in}_{HM,\theta\phi}=&\frac{1}{k^2}\sum_{l=1}^{\infty}\sum_{m=1}^{\infty}A_o\Big[\mp\sum_{\lambda=m}^{\infty}\frac{m}{(\kappa_p^2-k^2)I_{\lambda p}}\frac{1}{rr'sin\theta'}\Re'_\lambda(r)\Re'_\lambda(r')\Theta'_\lambda(\theta)\Theta_\lambda(\theta')\Phi_1(\phi)\Phi_2(\phi')\\&\pm\sum_{\mu=m}^{\infty}\frac{\kappa_q^{\ 2}}{(\kappa_q^2-k^2)I_{\mu q}}\frac{m}{sin\theta}\Re_\mu(r)\Re_\mu(r')\Theta_\mu(\theta)\Theta'_\mu(\theta')\Phi_2(\phi)\Phi_1(\phi')\Big]\end{aligned} \tag{4}$$

$$\begin{aligned}G^{in}_{HM,\phi\theta}=&\frac{1}{k^2}\sum_{l=1}^{\infty}\sum_{m=1}^{\infty}A_o\Big[\mp\sum_{\lambda=m}^{\infty}\frac{m}{(\kappa_p^2-k^2)I_{\lambda p}}\frac{1}{rr'sin\theta}\Re'_\lambda(r)\Re'_\lambda(r')\Theta_\lambda(\theta)\Theta'_\lambda(\theta')\Phi_2(\phi)\Phi_1(\phi')\\&\pm\sum_{\mu=m}^{\infty}\frac{\kappa_q^{\ 2}}{(\kappa_q^2-k^2)I_{\mu q}}\frac{m}{sin\theta'}\Re_\mu(r)\Re_\mu(r')\Theta'_\mu(\theta)\Theta_\mu(\theta')\Phi_1(\phi)\Phi_2(\phi')\end{aligned} \tag{5}$$

$$\begin{aligned}G^{in}_{HM,\phi\phi}=&\frac{1}{k^2}\sum_{l=1}^{\infty}\sum_{m=1}^{\infty}A_o\Big[\sum_{\lambda=m}^{\infty}\frac{m^2}{(\kappa_p^2-k^2)I_{\lambda p}}\frac{1}{rr'sin\theta sin\theta'}\Re'_\lambda(r)\Re'_\lambda(r')\Theta_\lambda(\theta)\Theta_\lambda(\theta')\Phi_2(\phi)\Phi_2(\phi')\\&+\sum_{\mu=m}^{\infty}\frac{\kappa_q^{\ 2}}{(\kappa_q^2-k^2)I_{\mu q}}\Re_\mu(r)\Re_\mu(r')\Theta'_\mu(\theta)\Theta'_\mu(\theta')\Phi_1(\phi)\Phi_1(\phi')\Big]\end{aligned} \tag{6}$$

$$\begin{aligned}G^{out}_{HM,\theta\theta}=&\frac{ik}{2}\sum_{m=1}^{\infty}\sum_{n=m}^{\infty}A_oB_{mn}\Big[\frac{1}{k^2rr'}\aleph'_n(r)[\Re'_n(r')+C_n\aleph'_n(r')]\Theta'_n(\theta)\Theta'_n(\theta')\Phi_1(\phi)\Phi_1(\phi')\\&\mp\frac{m^2}{sin\theta sin\theta'}\aleph_n(r)[\Re_n(r')+D_n\aleph'_n(r')]\Theta_n(\theta)\Theta_n(\theta')\Phi_2(\phi)\Phi_2(\phi')\Big]\end{aligned} \tag{7}$$

$$\begin{aligned}G^{out}_{HM,\theta\phi}=&\frac{ik}{2}\sum_{m=1}^{\infty}\sum_{n=m}^{\infty}A_oB_{mn}\Big[\mp\frac{1}{k^2rr'}\frac{m}{sin\theta'}\aleph'_n(r)[\Re'_n(r')\mp C_n\aleph'_n(r')]\Theta'_n(\theta)\Theta_n(\theta')\Phi_1(\phi)\Phi_2(\phi')\\&\pm\frac{m}{sin\theta}\aleph_n(r)[\Re_n(r')\pm D_n\aleph_n(r')]\Theta_n(\theta)\Theta'_n(\theta')\Phi_2(\phi)\Phi_1(\phi')\Big]\end{aligned} \tag{8}$$

$$\begin{aligned}G^{out}_{HM,\phi\theta}=&\frac{ik}{2}\sum_{m=1}^{\infty}\sum_{n=m}^{\infty}A_oB_{mn}\Big[\mp\frac{1}{k^2rr'}\frac{m}{sin\theta}\aleph'_n(r)[\Re'_n(r')\mp C_n\aleph'_n(r)]\Theta_n(\theta)\Theta'_n(\theta')\Phi_2(\phi)\Phi_1(\phi')\\&\pm\frac{m}{sin\theta'}\aleph'_n(r)[\Re_n(r')+D_n\aleph_n(r')]\Theta'_n(\theta)\Theta_n(\theta')\Phi_1(\phi)\Phi_2(\phi')\Big]\end{aligned} \tag{9}$$

$$\begin{aligned}G^{out}_{HM,\phi\phi}=&\mp\frac{ik}{2}\sum_{m=1}^{\infty}\sum_{n=m}^{\infty}A_oB_{mn}\Big[\frac{1}{k^2rr'}\aleph'_n(r)[\Re'_n(r')+C_n\aleph'_n(r')]\frac{m^2}{sin\theta sin\theta'}\Theta_n(\theta)\Theta_n(\theta')\Phi_2(\phi)\Phi_2(\phi')\\&+\aleph_n(r)[\Re_n(r')+D_n\aleph_n(r')]\Theta'_n(\theta)\Theta'_n(\theta')\Phi_1(\phi)\Phi_1(\phi')\Big]\end{aligned} \tag{10}$$

$$G^{in}_{HJ,\theta r}=\mp\sum_{l=1}^{\infty}\sum_{m=1}^{\infty}A_o\Big[\sum_{\mu=m}^{\infty}\frac{\mu(\mu+1)\kappa_q}{(\kappa_q^2-k^2)I_{\mu q}}\frac{m}{sin\theta}\Re_\mu(r)\Re_\mu(r')\Theta_\mu(\theta)\Theta_\mu(\theta')\Phi_2(\phi)\Phi_1(\phi')\Big] \tag{11}$$

$$G^{in}_{HJ,\phi r} = -\sum_{l=1}^{\infty}\sum_{m=1}^{\infty} A_o [\sum_{\mu=m}^{\infty} \frac{\mu(\mu+1)\kappa_q}{(\kappa_q^2 - k^2)I_{\mu q}} \Re_\mu(r)\Re_\mu(r')\Theta'_\mu(\theta)\Theta_\mu(\theta')\Phi_1(\phi)\Phi_1(\phi')] \quad (12)$$

$$G^{in}_{EM,r\theta} = \mp\sum_{l=1}^{\infty}\sum_{m=1}^{\infty} A_o [\sum_{\mu=m}^{\infty} \frac{\mu(\mu+1)\kappa_q}{(\kappa_q^2 - k^2)I_{\mu q}} \frac{m}{\sin\theta'} \Re_\mu(r)\Re_\mu(r')\Theta_\mu(\theta)\Theta_\mu(\theta')\Phi_1(\phi)\Phi_2(\phi')] \quad (13)$$

$$G^{in}_{EM,r\phi} = -\sum_{l=1}^{\infty}\sum_{m=1}^{\infty} A_o [\sum_{\mu=m}^{\infty} \frac{\mu(\mu+1)\kappa_q}{(\kappa_q^2 - k^2)I_{\mu q}} \Re_\mu(r)\Re_\mu(r')\Theta_\mu(\theta)\Theta'_\mu(\theta')\Phi_1(\phi)\Phi_1(\phi')] \quad (14)$$

$$G^{in}_{EJ,rr} = \frac{1}{k^2}[-\frac{1}{r^2\sin\theta}\delta(r-r')\delta(\theta-\theta')\delta(\phi-\phi') + \sum_{l=1}^{\infty}\sum_{m=1}^{\infty} A_o \sum_{\mu=m}^{\infty} \frac{\mu^2(\mu+1)^2}{(\kappa_q^2 - k^2)I_{\mu q}} \Re_\mu(r)\Re_\mu(r')\Theta_\mu(\theta)\Theta_\mu(\theta')\Phi_1(\phi)\Phi_1(\phi')] \quad (15)$$

where the common parameters can be defined as below and other notations have usual meaning as in references [4],[5].

$$\Re_\mu(r) = b_\mu(\kappa_p r),\ \Re'_\lambda(r) = \frac{\partial[rb_\lambda(\kappa_q r)]}{\partial r},\ \Re_n(r) = b_n(kr),\ \Re'_n(r) = \frac{\partial[rb_n(kr)]}{\partial r},\ \aleph_n(r) = h_n^{(1)}(kr),\ \aleph'_n(r) = \frac{\partial[rh_n^{(1)}(kr)]}{\partial r},$$

$$\Theta_\nu(\theta) = L_\nu^m(\cos\theta),\ \Theta'_\nu(\theta) = \frac{\partial L_\nu^m(\cos\theta)}{\partial\theta},\ \Phi_1(\phi) = \begin{cases}\cos\\ \sin\end{cases} m\phi,\ \Phi_2(\phi) = \begin{cases}\sin\\ \cos\end{cases} m\phi,\ A_o = \frac{2-\delta_o}{2\pi},\ B_{mn} = \frac{2n+1}{n(n+1)}\frac{(n-m)!}{(n+m)!},$$

$$C_n = -\frac{j_n(kR_b)}{h_n^{(1)}(kR_b)},\ D_n = \frac{[kR_b j_n(kR_b)]'}{[kR_b h_n^{(1)}(kR_b)]'}$$

$$I_{\upsilon\varsigma} = \frac{1}{\kappa_\varsigma\kappa'_\varsigma}\int_0^{\theta_c}\int_{R_a}^{R_b}\left\{\upsilon^2(\upsilon+1)^2 j_\upsilon(\kappa_\varsigma r) j_\upsilon(\kappa'_\varsigma r)[P_\varsigma^m(\cos\theta)]^2 + \frac{\partial[rj_\upsilon(\kappa_\varsigma r)]}{\partial r}\frac{\partial[rj_\upsilon(\kappa'_\varsigma r)]}{\partial r}\left[\left(\frac{\partial P_\varsigma^m(\cos\theta)}{\partial\theta}\right)^2 + \left(\frac{mP_\varsigma^m(\cos\theta)}{\sin\theta}\right)^2\right]\right\}\sin\theta\, dr\, d\theta$$

The following basis/testing functions on the slots $\hat{e}_{sk}$ and on the feed probe $\hat{j}_f$ are used, assuming the slots are narrow and the cavity is thin:

$$\hat{e}_{sk} = \hat{\zeta}_{sk} f_{sk}(\xi_{sk}) g_{sk}(\zeta_{sk}) = \hat{\zeta}_{sk} \frac{\sin\left\{k\left(\frac{l_{sk}}{2} - R_b|\xi_{sk}|\right)\right\}}{\sin\left(k\frac{l_{sk}}{2}\right)} \frac{1}{R_b\sqrt{\left(\frac{\varepsilon_{sk}}{2}\right)^2 - \zeta_{sk}^2}} \quad (16)$$

$$\hat{j}_f = \hat{r} \quad (17)$$

where l_{sk} and ε_{sk} are the length and the width of slot k, ξ_{sk} and ζ_{sk} are the local co-ordinates originating from the center of the k slot along the length and the width. By using the coordinate transformations as in [2] and solving the unknown currents, the antenna characteristics can be investigated from these currents.

4. Results

4.1 Impedance characteristics

The input impedance of the antenna can be found as the reciprocal of the coefficient a_f (input voltage of 1 V). From the antenna parameters illustrated in Table I, the result of the input impedance for various frequencies is shown in Fig.2. It is obvious that the theoretical results agreed satisfactory with the experimental ones. However, the bandwidth of VSWR≤*2* of experimental results is slightly narrower than the theoretical ones due to the imperfect of coaxial adapter in the measurement. However, the matching condition of this antenna must be improved which is left for further study.

Table I Antenna parameters used in the model

Slot length (*l*)	*0.5λ*
Slot width (α)	*0.017λ*
Outer spherical radius (R_b)	*1.43λ*
Inner spherical radius (R_a)	*1.27λ*
Shorted conical angle (θ_c)	*67.34°*
Center of slot pair angle (θ_c)	*40.00°*
Azimuthal spacing between slot pair (s_ϕ)	*0.481λ*
Elevation distance between slot in pair (d_θ)	*0.22λ*
Number of slot pair (*N*)	*12*

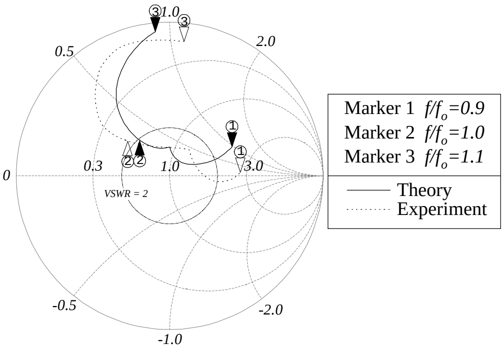

Fig.2 Input impedance

4.2 Radiation characteristics

Radiation characteristics such as radiation pattern of this antenna type is investigated by using the integration of the magnetic current sheets over all the slots and external dyadic Green's function together with the asymptotic expression of Hankel function for large argument, and the directivity is subsequently evaluated. Fig. 3 (a) and Fig.3 (b) illustrate the elevational and azimuthal patterns of the antenna, respectively. It is apparent that the antenna yields the conical beam radiation i.e., the elevation pattern possesses the null in broadside direction and the azimuthal pattern is omnidirectional. In addition, the elevational beam direction toward the geostationary satellite is relatively low which is suitable for applying to the land mobile subscriber unit located far from the equator. The directivity of *6.45* dBi at the maximum elevation angle of $60°$ is accomplished, that is sufficient for the application such as mobile satellite communication and wireless LAN base station. Experimental results are also set up to verify the theoretical results. It is obvious that the results of the elevational pattern are in good agreement. There are some errors expected from the edge diffraction and imperfect of the antenna fabrication. The azimuthal pattern at peak elevation angle between theoretical and experimental results are agreed very well.

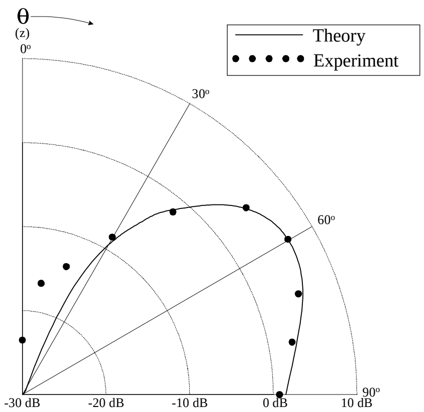

Fig.3 (a) Elevational pattern

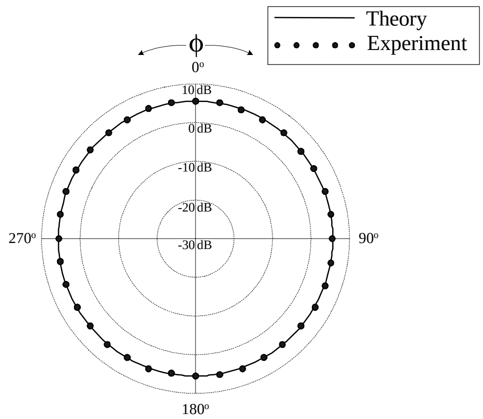

Fig.3 (b) Azimuthal pattern at $\theta=60°$

5. Conclusions

The impedance and radiation characteristics of a circularly polarized conical beam spherical slot array antenna are analyzed by using method of moments. The integral equations are constructed by imposing the boundary condition at the slots and feed probe. Dyadic Green's function derived from the boundary condition at the cavity is very useful aids in solving integral equations. Entire domain basis function with Galerkin's method of moments was selected to find the unknown currents. The result of the input impedance and radiation pattern is illustrated. To improve the result of the impedance characteristics, the slot length and cavity size must be varied to find the optimum condition, which is under investigations.

Acknowledgements

The first author would like to thank Prof. L. W. Li of the National University of Singapore for his helpful comments on the derivation the dyadic Green's function and Prof. J. Hirokawa of Tokyo Institute of Technology for his kind discussions.

References

[1] M.Krairiksh, C.Phongcharoenpanich, K.Meksamoot and J.Takada, "A circularly polarized conical beam spherical slot array antenna," *Int.J.Electronics*, vol.86, no.7, pp.815-823, July 1999.

[2] C.Phongcharoenpanich, M.Krairiksh and J.Takada, "Investigations of radiation characteristics of a circularly polarized conical beam spherical slot array antenna," *IEICE Trans.Electronics*, vol.E82-C, no.7, pp.1242-1247, July 1999.

[3] M.Ueno, S.Hosono, M.Takahashi, M.Ando and N.Goto, "Slot design of a concentric array radial line slot array antenna with matching terminating slots," *Proc. 1994 Asia-Pacific Microwave Conference*, pp.319-322, December 1994.

[4] C.Phongcharoenpanich, M.Krairiksh and J.Takada, "Dyadic Green's functions of a concentric conducting spherical cavity," *Proc.1997 Asia-Pacific Microwave Conference*, vol.2, pp.757-760, December 1997.

[5] C.T.Tai, *Dyadic Green Functions in Electromagnetic Theory*. New York: IEEE Press, 1993.